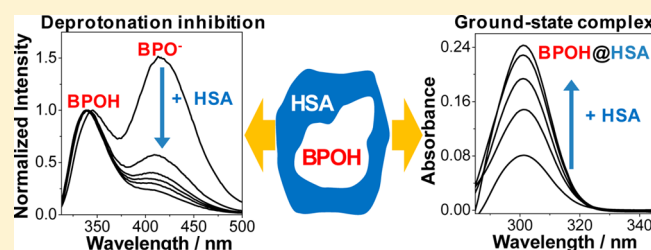


# Intraprotein Formation of a Long Wavelength Absorbing Complex and Inhibition of Excited-State Deprotonation in a Chiral Hydroxybiphenyl

Paula Bonancía, Ignacio Vayá, M. Consuelo Jiménez,\* and Miguel A. Miranda\*

Departamento de Química/Instituto de Tecnología Química UPV-CSIC, Universitat Politècnica de València, 46022 Valencia, Spain

**ABSTRACT:** The two enantiomers of 2-(2-hydroxybiphenyl-4-yl)propanoic acid ((S)- and (R)-BPOH) have been selected as probes for human serum albumin (HSA). Photophysical characterization in the absence of protein led to emission maxima, singlet energies, quantum yields, and fluorescence lifetime values of 332 nm, 91 kcal mol<sup>-1</sup>, and 0.28 and 1.8 ns for BPOH or 414 nm, 79 kcal mol<sup>-1</sup>, and 0.31 and 3.3 ns for the corresponding phenolate BPO<sup>-</sup>; the pK<sub>a</sub><sup>\*</sup> was found to be 1.17. In the presence of HSA, a light-absorbing ground-state complex (S)-BPOH@HSA was detected (maximum at ca. 300 nm) whose intensity increased with increasing protein concentration. The fluorescence spectra of (S)-BPOH in PBS, after addition of HSA, revealed a progressive diminution of the phenolate band, indicating that excited-state deprotonation is disfavored within the hydrophobic protein cavities. A similar trend was observed for (R)-BPOH, but the extent of deprotonation was significantly lower for this enantiomer. Addition of increasing amounts of the site II displacement probe (S)-ibuprofen ((S)-IBP) to BPOH@HSA led to a significant decrease of the absorption maximum at ca. 300 nm and to a recovery of the phenolate emission band at ca. 410 nm, which were again configuration dependent. The transient absorption spectrum of (S)-BPOH consisted on a broad band centered at 380 nm, attributed to the first triplet excited state. A dramatic enhancement of the triplet lifetimes within HSA was observed (19.0 μs within protein versus 1.3 μs in bulk PBS), although no stereodifferentiation was noticed in this case.



## INTRODUCTION

Transport proteins are responsible for carrying endogenous and exogenous agents in the bloodstream, for their delivery to specific targets. In particular, human serum albumin (HSA) is the most abundant transport protein in human blood and plasma, where it reaches concentrations of ca. 0.6 mM.<sup>1,2</sup> The three-dimensional structure of HSA has been determined crystallographically to a resolution of 2.8 Å. It is composed of 585 amino acids and comprises three homologous domains that assemble to form a heart-shaped molecule; each domain includes two subdomains that possess common structural motifs. The principal regions of ligand binding are located in hydrophobic cavities of subdomains IIA and IIIA (called by Sudlow sites I and II, respectively).<sup>3–5</sup> A large number of agents can be transported by HSA, including fatty acids and pharmaceutical drugs;<sup>6</sup> therefore, binding to HSA constitutes a key process, which is relevant for the modulation of a number of phenomena, such as drug solubility in plasma, toxicity, susceptibility to oxidation, in vivo half-life, etc.

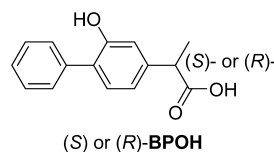
The binding sites of serum albumins provide an exceptional milieu, which can modify the physicochemical properties of the bound ligand. For example, the photophysics and photochemistry of some drugs,<sup>7</sup> dyes (rose bengal, methylene blue),<sup>8</sup> anthracene carboxylates<sup>9,10</sup> or propanoates,<sup>11</sup> naphthyl esters,<sup>12</sup> or diphenylamines<sup>13</sup> are strongly influenced by this medium.

In this context, the intrinsic photophysical properties of an encapsulated ligand can be employed to obtain relevant

information on the intraprotein microenvironment. Thus, from the quantum yields and lifetimes of the singlet or triplet excited states of a bound ligand, it is possible to determine key issues, such as the stoichiometry of the complex, the binding constant, or the extent of site occupation.<sup>14</sup>

For investigation of the specific characteristics of the protein binding sites, the proper choice of an appropriate ligand is essential. In this work, we have selected 2-(2-hydroxybiphenyl-4-yl)propanoic acid (BPOH, Chart 1) as probe, based on diverse structural and physicochemical considerations. Thus, BPOH is the main photoproduct of the nonsteroidal antiinflammatory drug flurbiprofen (FBP) in aqueous medium and is structurally related to the main FBP metabolite, 2-(2-fluoro-4'-hydroxy-4-biphenyl)propanoic acid.<sup>15</sup> It contains a biphenyl nucleus as active chromophore (that should generate

Chart 1. Chemical Structure of BPOH



Received: October 25, 2012

Revised: November 30, 2012

Published: December 3, 2012

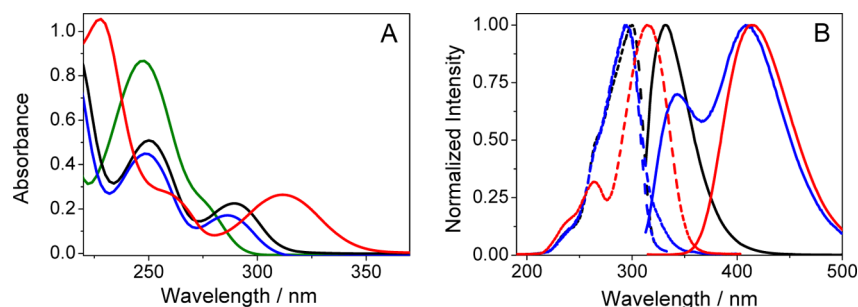


**Figure 1.** (A) UV absorption spectra of (S)-BPOH in MeCN (black), 0.01 M PBS (blue), and 0.1 M NaOH (red), together with that of (S)-FBP in MeCN (green) at  $5.5 \times 10^{-5}$  M concentration. (B) Normalized emission (solid lines,  $\lambda_{\text{exc}} = 308$  nm) and excitation spectra (dotted lines,  $\lambda_{\text{em}}$  at the corresponding maxima) of (S)-BPOH in MeCN (black), PBS (blue), and NaOH (red), under  $\text{N}_2$ .

short-lived species detectable by fluorescence or transient absorption spectroscopy). The presence of a hydroxy substituent results in a bathochromic shift of the absorption spectrum (which extends beyond 300 nm), with possible photobiological implications. Moreover, being a phenol, BPOH is expected to display a stronger acid character in the first singlet excited state ( $S_1$ ) than in the ground state ( $\text{p}K_{\text{a}}^* < \text{p}K_{\text{a}}$ ),<sup>16</sup> a useful property that can be employed to gather information on the nature of the microenvironment experienced by BPOH within the HSA binding sites. Finally, due to the presence of a chiral center, stereodifferentiation in the protein binding process is possible.

In this work, UV-absorption spectroscopy, as well as steady-state and time-resolved fluorescence combined with laser flash photolysis, has been applied to the study of BPOH in the absence and in the presence of HSA. The results provide clear evidence for intraprotein formation of a long wavelength absorbing complex and for inhibition of excited-state deprotonation.

## ■ EXPERIMENTAL SECTION

**Materials and Solvents.** (S)- and (R)-FBP, HSA, and (S)-IBP were commercially available. Their purity was checked by  $^1\text{H}$  nuclear magnetic resonance (NMR) and high-performance liquid chromatography (HPLC) analysis. Spectroscopic and HPLC-grade solvents were used without further purification. Solutions of phosphate-buffered saline (PBS) (0.01 M, pH = 7.4) were prepared by dissolving the commercial tablets in deionized water. The  $^1\text{H}$  NMR and  $^{13}\text{C}$  NMR spectra were recorded in  $\text{CDCl}_3$  as solvent at 300 and 75 MHz, respectively, using a Varian Gemini instrument; chemical shifts are reported in ppm. Isolation and purification were done by conventional column chromatography on silica gel Merck 60 (0.063–0.200 mm), or by preparative layer chromatography on silica gel Merck 60 F254, using hexane/ethyl acetate as eluents.

**Synthesis of (S)- and (R)-BPOH.**<sup>17</sup> A solution of (S)- or (R)-FBP (5 mM) in PBS was irradiated for 9 h through quartz, inside a Luzchem multilamp photoreactor, with the light from 10 8 W lamps emitting mainly at 254 nm. The photomixture was acidified with HCl, extracted with methylene chloride, and dried over  $\text{MgSO}_4$ . The organic layer was evaporated in vacuo and purified by preparative chromatography, using hexane/ethyl acetate, 40/60 (v/v), as eluent, affording (S)- or (R)-BPOH as white powder (60% yield).

**Preparation of the BPOH/HSA Samples.** For the studies in the presence of HSA, a battery of aqueous solutions containing (S)- or (R)-BPOH and HSA (molar ratios between 1:0.2 and 1:2) were prepared in neutral buffer (0.01 M PBS)

and stored for 15 h at 4 °C, to ensure a complete equilibrium between the ligand and the protein. The resulting solutions were placed in quartz cuvettes and submitted to fluorescence or laser flash photolysis experiments.

**Fluorescence Experiments.** Emission spectra were recorded on a JASCO FP-8500 spectrofluorometer system, provided with a monochromator in the wavelength range of 200–850 nm, and are uncorrected. Time-resolved measurements were performed with a TimeMaster fluorescence lifetime spectrometer TM-2/2003 from PTI by means of the stroboscopic technique, which is a variation of the boxcar technique. A hydrogen/nitrogen flashlamp was used as excitation source. The solutions were placed into 10 mm  $\times$  10 mm quartz cells. The absorbance of the samples at the excitation wavelength was kept below 0.2. Experiments were performed at 22 °C under air (in the presence of HSA) or  $\text{N}_2$ , as indicated in the figure legends.

**Laser Flash Photolysis Experiments.** The solutions of (S)- or (R)-BPOH and HSA at different molar ratios ( $A_{308} = 0.2$ ) were placed in a quartz cuvette and subjected to laser flash photolysis. In general, samples received between 5 and 10 pulses for all of the kinetic experiments. This light dose did not result in any detectable decomposition of the sample, as revealed by UV–vis absorption measurements prior to and after photolysis. Triplet lifetimes and fittings of the decay traces were coincident within the experimental error margins. To obtain the transient absorption spectra from 700 to 290 nm, a fresh sample was submitted to LFP at a regular interval of 10 nm (2 shots per wavelength). Experiments were carried out with a pulsed XeCl excimer laser ( $\lambda_{\text{exc}} = 308$  nm,  $\sim 17$  ns pulse width,  $< 100$  mJ per pulse). A pulsed Lo255 Oriel xenon lamp was used as a detecting light source. The observation wavelength was selected with a 77200 Oriel monochromator, and the signal was amplified by an Oriel photomultiplier tube (PMT) system made up of a 77348 side-on tube, 70680 housing, and a 70705 power supply. The signal was registered with a TDS-640A Tektronix oscilloscope and subsequently transferred to a personal computer. All experiments were done in  $10 \times 10$  mm<sup>2</sup> quartz cells with 4 mL capacity under air or  $\text{N}_2$ , as specified for each experiment in the figure legends.

**Phosphorescence Measurements.** Emission spectra were recorded on a spectrofluorometer system, which was provided with a monochromator in the wavelength range of 200–900 nm. The solutions were placed into a quartz tube and introduced into liquid nitrogen prior the measurements. The absorbance of the samples was 0.3 at the excitation wavelength (308 nm).

## RESULTS AND DISCUSSION

**Photophysical Behavior of (S)-BPOH in the Absence of Protein.** The UV absorption spectrum of (S)-BPOH in acetonitrile ( $5.5 \times 10^{-5}$  M) is shown in Figure 1A, together with that of (S)-FBP for comparison. As expected, replacement of the FBP fluorine by hydroxyl induces changes on the spectral properties of the chromophore; thus, the most salient feature in the (S)-BPOH spectrum is the presence of a well-defined band at relatively long wavelengths, which extends beyond 300 nm. The same trend was observed in phosphate buffered media (PBS 0.01 M, pH = 7.4). By contrast, the spectrum was clearly different in basic medium (0.1 M NaOH), which displayed a bathochromic shift, as expected for the corresponding phenolate (S)-BPO<sup>−</sup>.

The excitation and emission spectra of (S)-BPOH are shown in Figure 1B, whereas selected photophysical parameters are presented in Table 1. In acetonitrile, the fluorescence spectrum

**Table 1. Relevant Photophysical Parameters for (S)-BPOH in Acetonitrile and PBS at  $\lambda_{\text{exc}} = 308$  nm<sup>a</sup>**

solvent	$\phi_F$	$\lambda_{\text{em}}$ (nm)	$E_S$ (kcal mol <sup>−1</sup> ) <sup>b</sup>	$\tau_F$ (ns) <sup>b</sup>	$\tau_T$ ( $\mu$ s) <sup>b</sup>
MeCN	0.28	332	91	1.8	2
PBS	0.10	343/412	90/84	<1/3.3	13
NaOH	0.31	414	79	3.3	nd <sup>c</sup>

<sup>a</sup>All experiments were performed under N<sub>2</sub>. <sup>b</sup>Determined for the corresponding emission band(s). <sup>c</sup>Not determined.

consisted basically in a band centered at ca. 330 nm. The quantum yield ( $\phi_F$ ) was found to be 0.28, using carprofen in MeCN/N<sub>2</sub> as standard ( $\phi_F = 0.05$ ).<sup>18</sup> A singlet energy value ( $E_S$ ) of 91 kcal mol<sup>−1</sup> was obtained from the intersection between the excitation ( $\lambda_{\text{em}} = 330$  nm) and emission ( $\lambda_{\text{exc}} = 308$  nm) normalized bands. By contrast, the fluorescence spectrum in NaOH displayed a broad band centered at ca. 410 nm, corresponding to <sup>1</sup>((S)-BPO<sup>−</sup>)<sup>\*</sup>. The  $\phi_F$  and  $E_S$  values for this species were found to be 0.31 and 79 kcal mol<sup>−1</sup>, respectively. An intermediate behavior was observed in PBS, where the emission displayed two maxima, peaking at  $\lambda = 343$  and 412 nm, attributed to <sup>1</sup>((S)-BPOH)<sup>\*</sup> and <sup>1</sup>((S)-BPO<sup>−</sup>)<sup>\*</sup>, respectively. Besides, the coincidence of excitation spectra corresponding to both emission maxima in neutral aqueous medium indicates that (S)-BPOH is a photoacid, so under these conditions deprotonation is a singlet excited-state reaction. The  $pK_a^*$  value was estimated according to a Förster cycle,<sup>19</sup> using eq 1, where  $pK_a$  corresponds to the ground state,<sup>20</sup> and  $E_{S(\text{OH})}$  and  $E_{S(\text{O}^-)}$  are the singlet energies of phenol and phenolate (see above). The fact that the emission quantum

yield in PBS is markedly lower than in the organic solvent or in aqueous NaOH suggests that the excited phenol decays by an additional, nonradiative process in PBS (probably associated with hydrogen bonding).

$$pK_a^* = pK_a - \frac{E_{S(\text{OH})} - E_{S(\text{O}^-)}}{2.303RT} \quad (1)$$

With these data, the  $pK_a^*$  value was found to be 1.17, indicating a clearly stronger acidity of (S)-BPOH in the first singlet excited state than in the ground state. This is in good agreement with the reported value of  $pK_a^* = 1.15$  for the closely related compound 2-hydroxybiphenyl.<sup>21</sup>

The fluorescence lifetimes ( $\tau_F$ ) at the emission maxima are given in Table 1. When comparing MeCN with PBS, the  $\tau_F$  of the free phenol dropped dramatically in the latter medium (from 1.8 ns to less than 1 ns), indicating a strong dynamic quenching. By contrast, a  $\tau_F$  value of 3.3 ns was obtained for the phenolate at  $\lambda_{\text{em}} = 412$  nm, both in PBS and in alkaline solution.

The transient absorption spectrum of (S)-BPOH obtained upon laser flash photolysis ( $\lambda_{\text{exc}} = 308$  nm, MeCN/N<sub>2</sub>), consisted on a broad band centered at 380 nm, which was attributed to the first triplet excited state, by comparison with literature data for 2-hydroxybiphenyl.<sup>22</sup> It is shown in Figure 2A, together with the decay trace monitored at  $\lambda_{\text{em}} = 380$  nm (inset, Figure 2A). The spectrum was similar in PBS, although <sup>3</sup>(S)-BPOH<sup>\*</sup> was markedly longer lived ( $\tau_T = 13$   $\mu$ s in PBS versus 2  $\mu$ s in MeCN).

As expected, <sup>3</sup>(S)-BPOH<sup>\*</sup> was quenched by O<sub>2</sub> ( $k_Q = 2.2 \times 10^9$  M<sup>−1</sup> s<sup>−1</sup> in PBS). Additional information on the triplet excited state was obtained by recording the phosphorescence spectrum of (S)-BPOH in ethanol matrix at 78 K (Figure 2B). With this data, the <sup>3</sup>(S)-BPOH<sup>\*</sup> energy was determined as 65 kcal mol<sup>−1</sup>, quite comparable with that of FBP.

**Studies on (S)- and (R)-BPOH/HSA Systems.** After characterization of the photophysical properties of (S)-BPOH in organic and aqueous media, the studies were extended to (S)-BPOH and (R)-BPOH in the presence of HSA. The availability of the two enantiomers allowed us to look for a possible stereodifferentiation in the photophysical behavior of the ligand after encapsulation within the protein binding sites. The solutions were prepared in air-equilibrated PBS to avoid foam formation associated with nitrogen bubbling.

Figure 3A shows the absorption spectra of equimolar (S)-BPOH/HSA mixtures (10<sup>−4</sup> M in PBS), together with those of the separated components. For comparison, a theoretical curve obtained by addition of the traces corresponding to (S)-BPOH and HSA is also represented. The mismatch between the

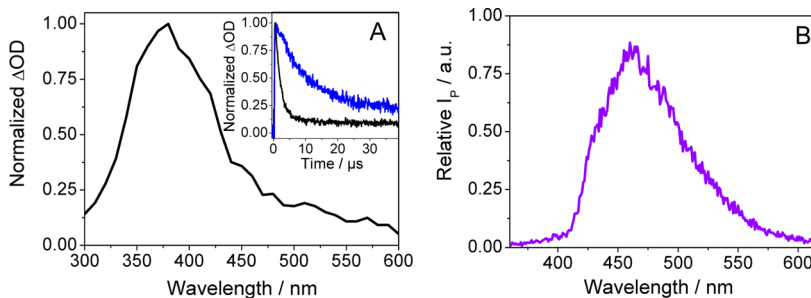


**Figure 2.** (A) Transient absorption spectrum 0.9  $\mu$ s after the laser pulse of (S)-BPOH ( $2 \times 10^{-4}$  M) in deaerated MeCN solution ( $\lambda_{\text{exc}} = 308$  nm). Inset: Normalized decay traces monitored at 380 nm in MeCN (black) and PBS (blue). (B) Phosphorescence spectrum in ethanol matrix.

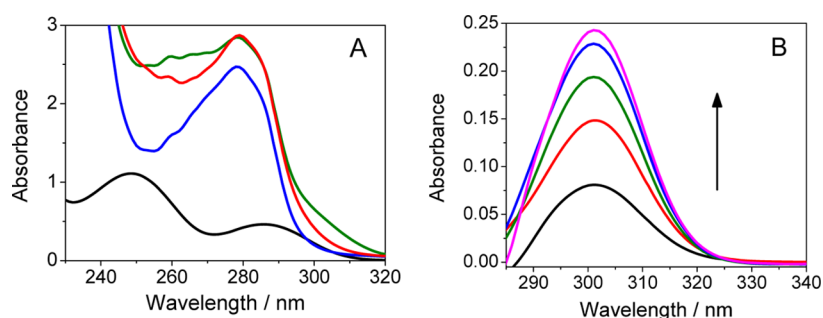


**Figure 3.** (A) UV absorption spectra (in PBS) of (S)-BPOH (black), HSA (blue), and an equimolar (S)-BPOH/HSA mixture (green), together with a simulated curve obtained as (S)-BPOH + HSA (red). The concentration of each component was  $10^{-4}$  M. (B) Curves obtained as (S)-BPOH/HSA–(S)-BPOH/HSA at different (S)-BPOH/HSA molar ratios: black, 1:0.2; red, 1:0.4; green, 1:0.6; blue, 1:0.8; magenta, 1:1.

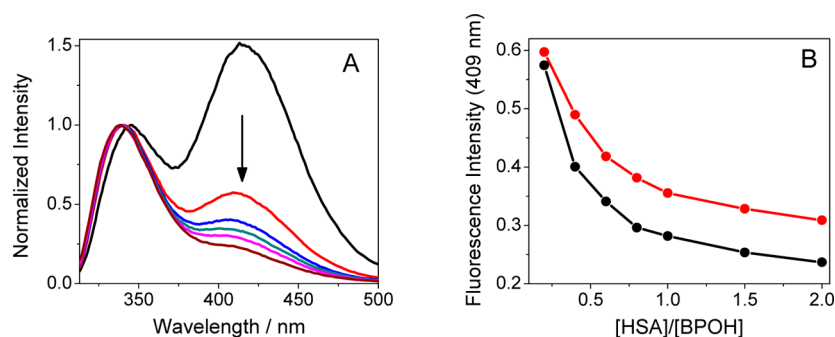


**Figure 4.** (A) Fluorescence spectra (normalized at the short-wavelength maximum) of (S)-BPOH in PBS ( $\lambda_{\text{exc}} = 308$  nm, air,  $10^{-4}$  M) after addition of increasing amounts of HSA. The (S)-BPOH/HSA molar ratios are 1:0 (black), 1:0.2 (red), 1:0.4 (blue), 1:0.6 (green), 1:0.8 (magenta), and 1:2 (brown). (B) Plot of the fluorescence intensity at 409 nm vs HSA/BPOH molar ratio for (S)-BPOH (black) and (R)-BPOH (red).

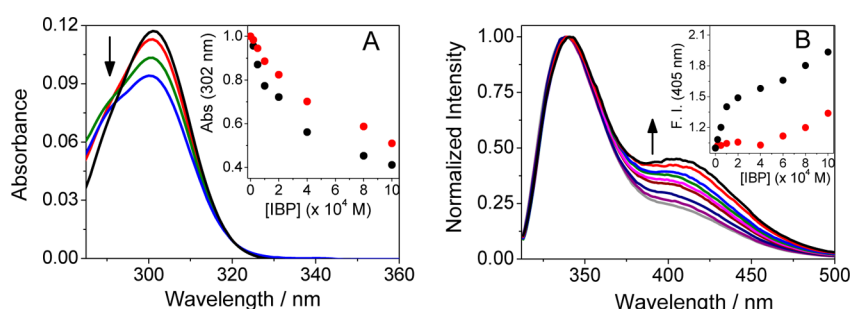


**Figure 5.** (A) Differential UV absorption curves of the ground state complex obtained as (S)-BPOH/HSA–(S)-BPOH–HSA–(S)-IBP in the presence of increasing amounts of (S)-IBP. Molar ratios (S)-BPOH/HSA/(S)-IBP: 1:1.4:1 (blue), 1:1.4:0.5 (green), 1:1.4:0.2 (red), 1:1.4:0 (black). Inset: Plot of the absorbance at 302 nm vs (S)-IBP concentration for (S)-BPOH/HSA (black) and (R)-BPOH/HSA (red). (B) Normalized fluorescence spectra of (S)-BPOH/HSA systems after addition of increasing amounts of (S)-IBP. Inset: Plot of the fluorescence intensity at 405 nm vs IBP concentration for (S)-BPOH/HSA (black) and (R)-BPOH/HSA (red). For parts A and B, [BPOH] was  $10^{-4}$  M and BPOH/HSA molar ratio was 1:1.4 in all cases.

experimental and theoretical results clearly reveals formation of a light absorbing ground-state complex in the region 290–330 nm. For its characterization, a series of (S)-BPOH/HSA solutions at different molar ratios were prepared. The spectral curves obtained by subtraction of isolated (S)-BPOH and HSA from the corresponding mixtures are shown in Figure 3B. Operating in this way, clear absorption maxima emerged at ca. 300 nm, whose intensity increased with increasing protein concentration; they were ascribed to the (S)-BPOH@HSA complex.

The fluorescence spectra of  $10^{-4}$  M (S)-BPOH in PBS, after addition of increasing amounts of HSA, are shown in Figure 4A. The most remarkable observation was the progressive diminution of the phenolate band inside the protein, indicating that excited-state deprotonation is disfavored within the

hydrophobic HSA cavities. In addition, the emission maximum in PBS was slightly red-shifted, due to the lower polarity experienced within the protein. A similar trend was observed for (R)-BPOH; however, it was interesting to realize that the extent of deprotonation was significantly lower for this enantiomer under identical conditions (Figure 4B).

In order to obtain additional experimental evidence supporting formation of a light-absorbing ground-state complex, the UV-spectral changes of 1:1.4 BPOH/HSA mixtures were monitored upon addition of a displacement probe. Taking into account that the parent drug FBP binds mainly to site II of HSA and that the presence of an additional hydroxy group in BPOH should even enhance this preference, (S)-ibuprofen ((S)-IBP) was selected as displacement probe.<sup>4</sup> In the presence of (S)-IBP, a lower contribution of the



complexed BPOH form should be found, concomitantly with the presence of more BPOH in the bulk solution. In the UVspectra, this would result in a diminished intensity of the long-wavelength absorption band. As a matter of fact, when the differential spectra of the samples were obtained (Figure 5A), the maximum at ca. 300 nm exhibited a significant decrease with increasing concentrations of (S)-IBP, which was configuration dependent (inset of Figure 5A). In parallel, the fluorescence changes were recorded for the same samples, revealing that displacement of BPOH by (S)-IBP from the protein microenvironment to the solution, where deprotonation is enhanced, leads to a recovery of the phenolate emission band (Figure 5B). Again, a significant stereodifferentiation was observed for this process (inset of Figure 5B).

Finally, the emission decays at 330 nm ( $\lambda_{\text{exc}} = 308$  nm) in the presence of HSA occurred within less than 1 ns. By contrast, the kinetics of triplet decay obtained by laser flash photolysis revealed a dramatic enhancement of the  $\tau_T$  values within HSA (19.0  $\mu\text{s}$  in protein versus 1.3  $\mu\text{s}$  in bulk PBS, under air), although no stereodifferentiation was observed in this case.

## CONCLUSIONS

Photophysical studies including UV-absorption spectroscopy and steady-state and time-resolved fluorescence, as well as laser flash photolysis, have been applied to the study of the two enantiomers of BPOH in the absence and in the presence of HSA. Intraprotein formation of a long wavelength absorbing complex BPOH@HSA is associated with the appearance of a new absorption band at ca. 300 nm, whose intensity increases with increasing protein concentration and decreases upon addition of (S)-IBP, a site II displacement probe. Fluorescence measurements provide clear evidence for inhibition of excited-state deprotonation within the hydrophobic protein binding sites, as revealed by the marked diminution of the phenolate band (at  $\lambda_{\text{em}}$  ca. 410 nm) in the presence of HSA. A significant stereodifferentiation is observed both in formation of the ground-state complex and in excited state deprotonation.

## AUTHOR INFORMATION

### Corresponding Author

\*E-mail: mmiranda@qim.upv.es (M.A.M.); mcjimene@qim.upv.es (M.C.J.). Phone: +34963877344. Fax: +34963879349.

### Notes

The authors declare no competing financial interest.

## ACKNOWLEDGMENTS

Financial support from the Spanish Government (CTQ2010-14882, CTQ2009-13699, BES-2008-003314, JCI-2011-09926), from the Generalitat Valenciana (Prometeo 2008/090) and from the Universitat Politècnica de València (PAID 05-11, 2766) is gratefully acknowledged.

## REFERENCES

- (1) Peters, T. *All About Albumins: Biochemistry Genetics and Medical Applications*; Academic Press: San Diego, CA, 1995.
- (2) Carter, D. C.; Ho, J. X. in *Advances in Protein Chemistry*; Academic Press: New York, 1994; Vol. 45, pp 152–203.
- (3) Sudlow, G.; Birkett, D. J.; Wade, D. N. *Mol. Pharmacol.* **1975**, *11*, 824–832.
- (4) Sudlow, G.; Birkett, D. J.; Wade, D. N. *Mol. Pharmacol.* **1976**, *12*, 1052–1061.
- (5) He, X. M.; Carter, D. C. *Nature* **1992**, *358*, 209–215.
- (6) Krag-Hansen, U. *Dan. Med. Bull.* **1990**, *37*, 57–84.

- (7) Lhiaubet-Vallet, V.; Sarabia, Z.; Boscá, F.; Miranda, M. A. *J. Am. Chem. Soc.* **2004**, *126*, 9538–9539.
- (8) Alarcón, E.; Edwards, A. M.; Aspee, A.; Moran, F. E.; Borsarelli, C. D.; Lissi, E. A.; González-Nilo, D.; Poblete, H.; Scaiano, J. C. *Photochem. Photobiol. Sci.* **2010**, *9*, 93–102.
- (9) Nishijima, M.; Wada, T.; Mori, T.; Pace, T. C. S.; Bohne, C.; Inoue, Y. *J. Am. Chem. Soc.* **2007**, *129*, 3478–3479.
- (10) Wada, T.; Nishijima, M.; Fujisawa, T.; Sugahara, N.; Mori, T.; Nakamura, A.; Inoue, Y. *J. Am. Chem. Soc.* **2003**, *125*, 7492–7493.
- (11) Alonso, R.; Jiménez, M. C.; Miranda, M. A. *Org. Lett.* **2011**, *13*, 3860–3863.
- (12) Marin, M.; Lhiaubet-Vallet, V.; Miranda, M. A. *J. Phys. Chem. B* **2011**, *115*, 2910–2915.
- (13) Marin, M.; Lhiaubet-Vallet, V.; Miranda, M. A. *Org. Lett.* **2012**, *14*, 1788–1791.
- (14) Alonso, R.; Yamaji, M.; Jiménez, M. C.; Miranda, M. A. *J. Phys. Chem. B* **2010**, *114*, 11363–11369.
- (15) Adams, W. J.; Bothwell, B. E.; Bothwell, W. M.; VanGiessen, G. J.; Kaiser, D. G. *Anal. Chem.* **1987**, *59*, 1504–1509.
- (16) Bartok, W. P.; Lucchesi, J.; Snider, N. S. *J. Am. Chem. Soc.* **1962**, *84*, 1842–1844.
- (17) Jiménez, M. C.; Miranda, M. A.; Tormos, R.; Vayá, I. *Photochem. Photobiol. Sci.* **2004**, *3*, 1038–1041.
- (18) Asíns-Fabra, B.; Andreu, I.; Jiménez, M. C.; Miranda, M. A. *J. Photochem. Photobiol. A* **2009**, *207*, 52–57.
- (19) Förster, T. *Z. Electrochem.* **1950**, *54*, 531–553.
- (20) The  $\text{pK}_a$  of 2-hydroxybiphenyl has been employed for the calculations. It was taken from: Bridges, J. W.; Creaven, P. J.; Williams, R. T. *Biochem. J.* **1965**, *96*, 872–878.
- (21) Lukeman, M.; Wan, P. *J. Am. Chem. Soc.* **2002**, *124*, 9458–9464.
- (22) Mohana, H.; Bredeb, O.; Mittal, J. P. *J. Photochem. Photobiol. A* **2001**, *140*, 191–197.